Fabrication of 6.5 m f/1.25 Mirrors for the MMT and Magellan Telescopes

H. M. Martin, R. G. Allen, J. H. Burge, L. R. Dettmann, D. A. Ketelsen, W. C. Kittrell, S. M. Miller and S. C. West
Steward Observatory, University of Arizona, Tucson, AZ 85721

Abstract

We describe the fabrication of the 6.5 m f/1.25 primary mirrors for the Multiple Mirror Telescope Conversion and the first Magellan telescope. Figuring was performed with a 1.2 m stressed lap–which bends under active control to match the local curvature of the optical surface–and small passive tools. The figure was measured with IR and visible interferometers, using refractive null correctors to compensate 810 microns of aspheric departure. We present the final measurements as surface maps, synthetic interferograms and synthetic images.

Keywords

(350.1260) Astronomical optics; (110.6770) Telescopes; (220.4610) Optical fabrication; (220.4840) Optical testing.

Introduction

The primary mirrors for the Multiple Mirror Telescope (MMT) Conversion and the first Magellan telescope are the first large honeycomb sandwich mirrors cast and polished by the Steward Observatory Mirror Lab. The MMT on Mt. Hopkins in southern Arizona is being converted to a single-mirror telescope, with a 6.5 m primary mirror replacing its six 1.8 m mirrors. [1] Going to a filled aperture doubles the collecting area and increases the 2-D field of view by a factor of 200. The two 6.5 m Magellan telescopes are under construction on Las Campanas in Chile. [2] The primary mirrors for the three telescopes are identical f/1.25 paraboloids.

The MMT mirror is shown in Figure 1. It is a honeycomb sandwich with a maximum thickness of 0.71 m and lightweighted by a factor of 5, giving a very stiff and thermally responsive mirror. The concave front shell and flat back plate are 25-28 mm thick, and these are separated by 12 mm ribs in a hexagonal pattern with 192 mm spacing. The short focal length allows use of a compact and economical enclosure and keeps the secondary support structure short and stiff.

Figure 1. MMT primary mirror, viewed from the back, on its turning frame.

Such fast mirrors present the challenge of polishing the extremely aspheric surface, and the accuracy requirements are stringent, especially at small spatial scales. The error budget matches the wavefront distortion induced by the atmosphere, and the allowed errors increase with spatial scale. The Mirror Lab's polishing system is designed to give small-scale smoothness on aspheric surfaces. Most lapping operations are performed with a stressed lap that

maintains fit through continuous active shape changes. [3,4] The lap is relatively large (1.2 m) and stiff in order to provide strong passive smoothing.

Fabrication

The casting and generating processes are described elsewhere. [5,6] For loose-abrasive grinding and polishing we use the same stressed lap, shown in Figure 2. It is a 1.5 m aluminum plate, 50 mm thick, with 18 moment-generating actuators around its edge to bend it elastically. Three more actuators apply lifting forces to control polishing pressure and pressure gradients. The polishing surface is 1.2 m in diameter. The bending actuators are programmed to make the lap shape match the ideal parabolic mirror surface at all times, while the lifting actuators can be used to vary the pressure according to the current figure error—applying more pressure at the high points—and to balance forces when the lap extends over the edge of the mirror.

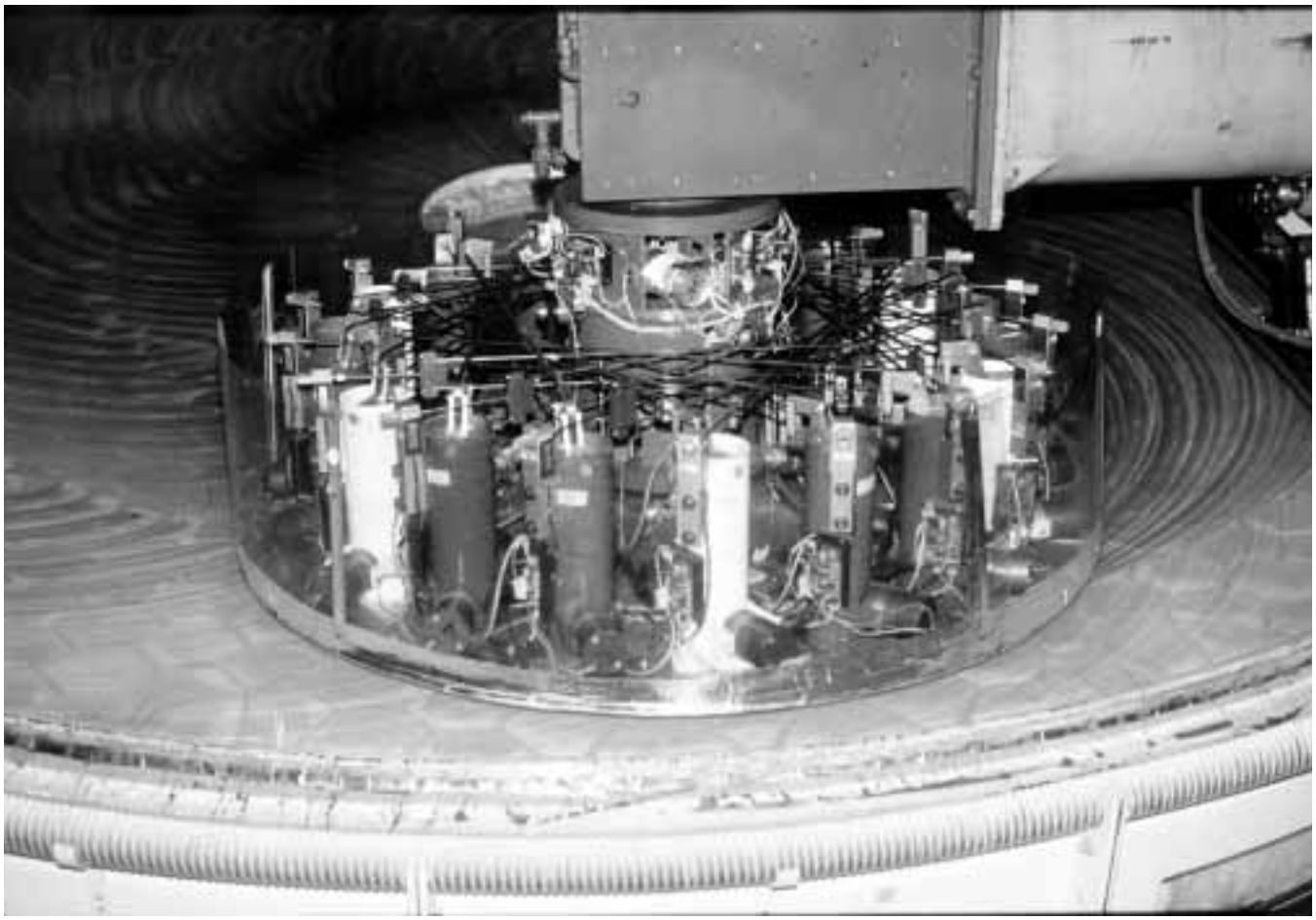

Figure 2. Stressed lap in use on the MMT mirror.

Horizontal forces and torque are transmitted to the lap through three linkages that attach tangentially and allow it to move vertically and tilt. While polishing the MMT mirror we discovered that the linkages occasionally bound at the extreme edge tilt of $11°$, causing large uncontrolled pressure gradients. This may have caused some non-axisymmetric figure errors that were only partially corrected by subsequent polishing after the problem was fixed.

The polishing machine, shown in Figure 3, provides dynamic control of the speeds of its three polishing motions (radial, mirror rotation and lap rotation). We generally use the radial motion and lap rotation to control axisymmetric figure errors. Variations in pressure and mirror rotation rate can be used to remove non-axisymmetric errors. We control print-through of the honeycomb structure under polishing pressure by applying an equal air pressure to the inside of the mirror.

In addition to the stressed lap, we use stiff passive tools from 10 to 40 cm in diameter for local figuring. Short radial

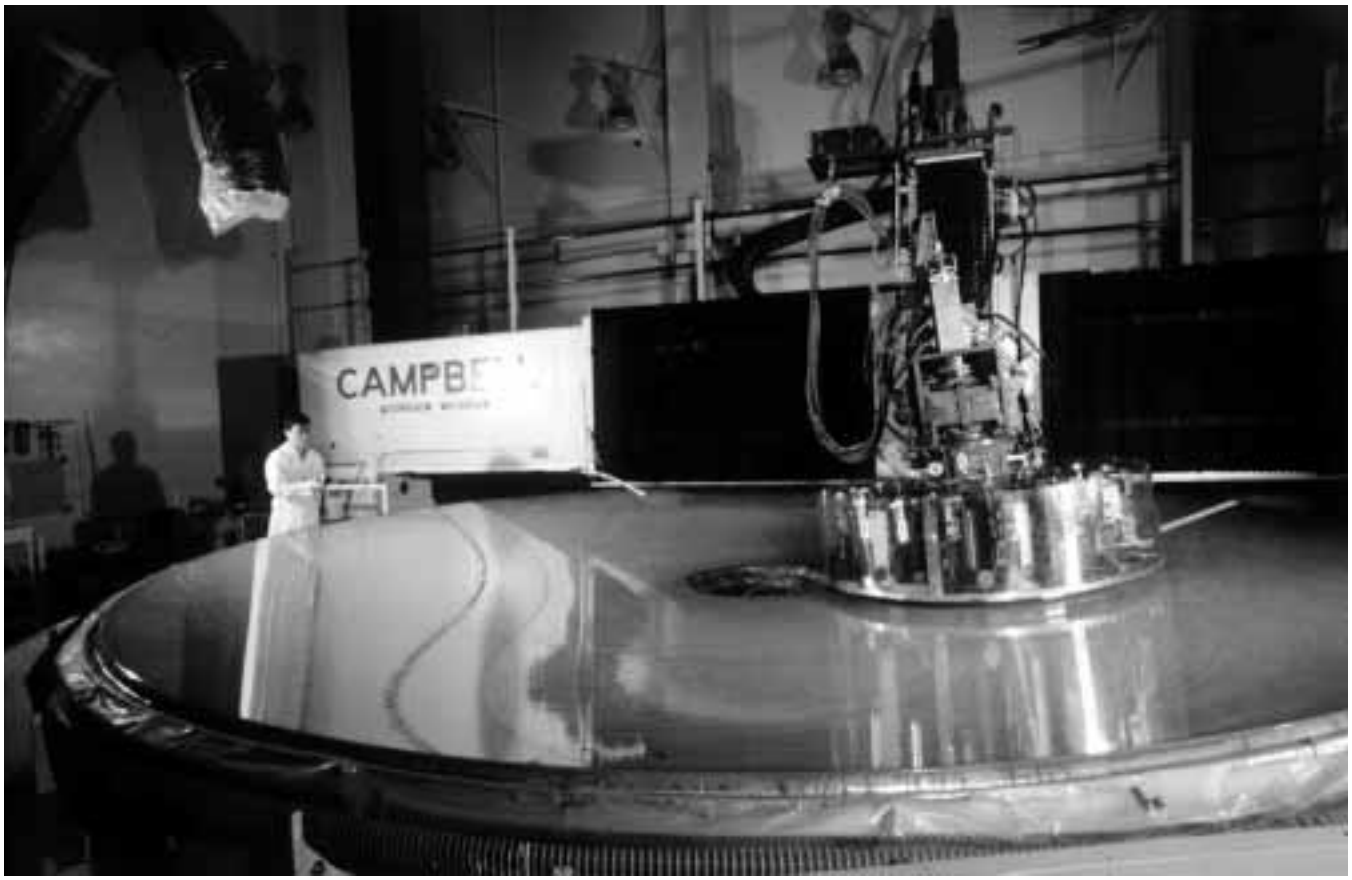

Figure 3. MMT primary mirror being polished.

strokes are used in order to limit misfit between the lap and the aspheric surface.

Optical measurements

All lapping operations are guided by phase-shifting interferometry. We use a 10.6 micron interferometer for loose-abrasive grinding and early polishing, and a 531 nm interferometer for the final figuring. Both interferometers are sensitive to surface errors of about $\lambda/100$. Separate IR and visible null lenses correct the 810 micron departure from the best-fitting sphere.

We measure the accuracy of both null lenses using small computer-generated holograms that simulate the ideal primary mirror. [7] Measurement of the visible hologram with the visible null lens revealed a discrepancy of 150 nm of spherical aberration (surface Zernike coefficient), equivalent to 2.7×10^{-4} in conic constant. After verifying the mechanical dimensions and surface figures of the null lens, we eventually traced the problem to an error in refractive index in the largest element, which is 55 mm thick. We figured the mirrors using the hologram as the standard for spherical aberration.

Mirror support

The mirror support cell used for polishing and testing simulates the telescope support, with 104 support points most of which are distributed through 2- or 3-point loadspreaders. While the telescope supports are active pneumatic actuators, the laboratory system uses passive hydraulic cylinders.

We monitored support forces at the 104 support locations and found that they varied by about 5 N rms during work on the MMT mirror and slightly less for the Magellan mirror. The force variations probably come from a combination of leakage and friction in the passive hydraulic supports. Some problems with the cylinder mechanism were identified and fixed before we completed the Magellan mirror. These force variations are expected to produce astigmatism (by far the most flexible bending mode) on the order of 300 nm peak-to-valley surface, and smaller amounts of other flexible modes. Variations of this magnitude were observed from day to day. Larger errors in support forces during the loose-abrasive grinding of the MMT mirror led to about 1 micron peak-to-valley astigmatism present in the polished surface at the time of the first visible measurements. We decided to correct this with the active supports in the telescope rather than by polishing it out. These ampli-

tudes of flexible bending modes have no effect on telescope performance, as they will be controlled by the active support system. [8]

Results

We present the final results in the form of surface contour maps and synthetic interference patterns for both mirrors, and include diffraction calculations for the Magellan mirror. All data are based on an average of about 50 phase maps. The noise in an individual map, caused primarily by turbulence, averages about 50 nm rms surface error and shows little or no correlation between maps. The noise in the average should be less than 10 nm rms. Tilt, focus and coma, which result from slight misalignment of the interferometer with respect to the optical axis of the mirror, have been subtracted.

Figures 4-6 show the surface contour maps and synthetic interferograms. Astigmatism and a small amount of spherical aberration have been subtracted from all data shown. Spherical aberration in the telescope will be determined by the spacing of the optics. For the MMT mirror we also show results after subtracting two additional flexible modes that will be corrected by the active supports in the telescope. The amplitudes of the subtracted aberrations are listed in Table 1.

Figure 4. Gray-scale map of the mirror surface and synthetic interferogram for the MMT mirror with astigmatism and spherical aberration subtracted. The gray scale covers ±100 nm of surface and the rms surface error is 35 nm. The interferogram is calculated for a wavelength of 531 nm.

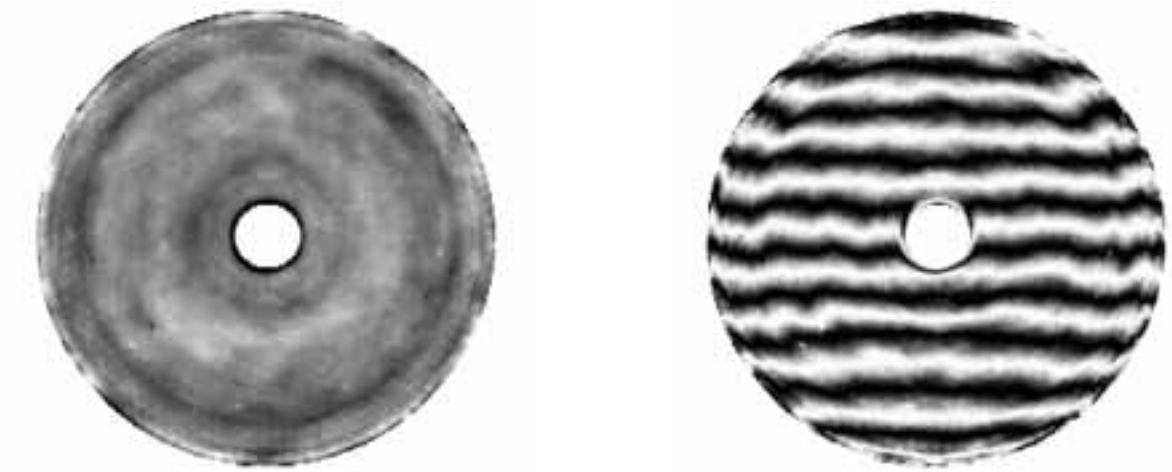

Figure 5. Same as Figure 4 except that two additional flexible bending modes have been subtracted. The rms surface error is 26 nm.

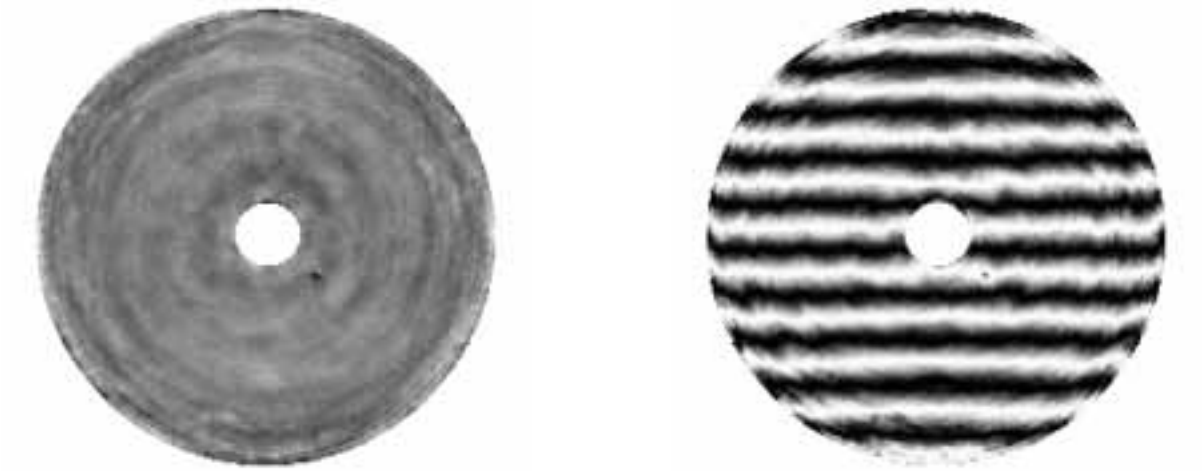

Figure 6. Gray-scale map of the mirror surface and synthetic interferogram for the Magellan mirror with astigmatism and spherical aberration subtracted. The gray scale covers ±100 nm of surface and the rms surface error is 14 nm. The interferogram is calculated for a wavelength of 531 nm.

Table 1: Low-order aberrations subtracted (Zernike coefficient in nm of surface)

aberration	MMT	Magellan
astigmatism	530	270
spherical aberration	14	40
trefoil	32	
5^{th} order astigmatism	55	

We calculated synthetic images from the measured wavefronts. Figure 7 shows the point-spread functions of the actual Magellan mirror and a perfect mirror. Figure 8 shows encircled energy diagrams for the Magellan mirror in a perfect atmosphere and in 0.25″ seeing (slightly better than we ever expect to see). In perfect seeing the mirror focuses 80% of the light at 500 nm into a 0.06″ diameter.

Discussion

Both mirrors will form excellent images and contribute negligible errors to the wavefront in the best seeing. The Magellan mirror is more accurate on spatial scales between about 10 cm and 1 m. Factors contributing to the difference include:

1. improvements in the stressed lap hardware, eliminating some uncontrolled variations in polishing pressure and pressure gradients;
2. improvements in mirror supports, giving smaller force errors;
3. more experience with the polishing system.

The Mirror Lab will polish another 6.5 m mirror for the second Magellan telescope, followed by two 8.4 m f/1.14 mirrors for the Large Binocular Telescope. [9]

References

1. S. C. West, *et al*., "Toward first light for the 6.5-m MMT Telescope", in *Optical Telescopes of Today and Tomorrow: Following in the Direction of Tycho Brahe*, A. Ardeberg, ed., Proc. SPIE 2871, p. 38 (1996).
2. M. Johns, "Magellan 6.5-m telescopes project: status report", in *Advanced Technology Optical/IR Telescopes VI*, L. M. Stepp, ed., Proc. SPIE 3352, p. 102 (1998).
3. H. M. Martin, *et al*., "Progress in the stressed-lap polishing of a 1.8-m f/1 mirror", in *Advanced Technology Optical Telescopes IV*, L. D. Barr, ed., Proc. SPIE 1236, p. 682 (1990).
4. S. C. West, *et al*., "Practical Design and Performance of the Stressed-Lap Polishing Tool", *Applied Optics* 33, p. 8094 (1994).
5. B. H. Olbert, J. R. P. Angel, J. M. Hill and S. F. Hinman, "Casting 6.5-meter mirrors for the MMT conversion and Magellan", in *Advanced Technology Optical Telescopes V*, L. M. Stepp, ed., Proc. SPIE 2199, p. 144 (1994).
6. H. M. Martin, J. H. Burge, D. A. Ketelsen and S. C. West, "Fabrication of the 6.5 m primary mirror for the Multiple Mirror Telescope Conversion", in *Optical Telescopes of Today and Tomorrow: Following in the Direction of Tycho Brahe*, A. Ardeberg, ed., Proc. SPIE 2871, p. 399 (1997).

Figure 7. Synthetic images at 0.5 micron for the actual Magellan mirror of Figure 6 (left) and a perfect mirror (right). The images are separated by 0.5″.

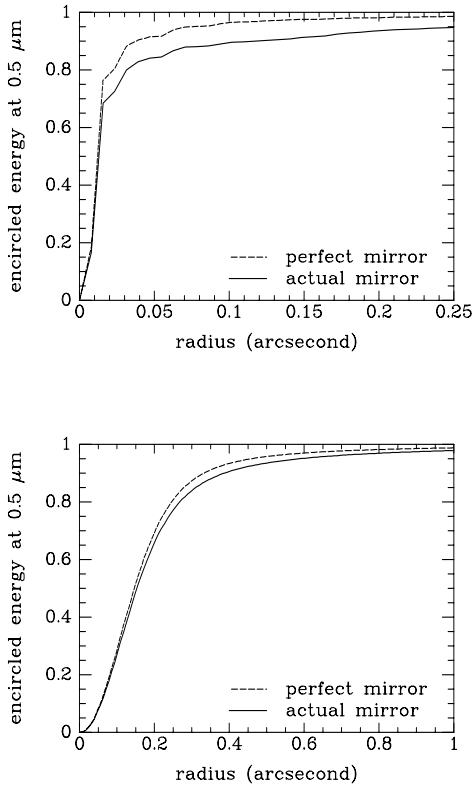

Figure 8. Encircled energy as a function of radius for the Magellan mirror and for a perfect mirror. Top: in perfect seeing. Bottom: in seeing of 0.25″ FWHM.

7. J. H. Burge, D. S. Anderson, D. A. Ketelsen and S. C. West, “Null test optics for the MMT and Magellan 6.5-m f/1.25 primary mirrors”, in *Advanced Technology Optical Telescopes V*, L. M. Stepp, ed., Proc. SPIE 2199, p. 658 (1994).
8. H. M. Martin, *et al.*, “Active supports and force optimization for the MMT primary mirror”, in *Advanced Technology Optical/IR Telescopes VI*, L. M. Stepp, ed., Proc. SPIE 3352, p. 412 (1998).
9. J. M. Hill and P. Salinari, “Large Binocular Telescope Project”, *ibid*, p. 23.